Neurogastroenterol Motil (2004) **16,** 475–487 doi: 10.1111/j.1365-2982.2004.00565.x

Changes in nitrergic innervation of defunctionalized rat colon after diversion colostomy

A. CHAUDHURY,* A. SHARIFF,* M. SRINIVAS† & U. SABHERWAL*

*Department of Anatomy, All India Institute of Medical Sciences (AIIMS), New Delhi, India
†Department of Pediatric Surgery, All India Institute of Medical Sciences (AIIMS), New Delhi, India

Abstract *After 45 days of complete diversion colostomy in male Wistar rats, morphometry of soma and nuclei of NADPH diaphorase positive cells of the myenteric plexus was evaluated. There was a significant ($P < 0.0001$) diminution in the area, perimeter and volume-weighted mean volume of soma and nuclei of nitrergic myenteric neurones in the defunctionalized colon. In addition, there was a significant reduction in the neuronal density of the myenteric neurones, and increased distance between the ganglia. In addition, there was myenteric glial atrophy. Atrophy of colonic myenteric neurones was accompanied by significant reduction ($P < 0.001$) in the volume fraction of the muscularis externa, the prime targets of these neurones. The disturbances in the microecology of the colon may jeopardize the finely orchestrated functioning of the components of the Enteric nervous system (ENS) leading to colonic dysfunction. Our observations, by extrapolation, may explain the bowel dysmotility in humans after restoration of colonic continuity after colostomy.*

Keywords *diversion colostomy, enteric nervous system, myenteric neurones, nitrergic, plasticity, stereology.*

INTRODUCTION

Colostomy is performed as the first step in multistage procedures for congenital abnormalities like Hirschsprung's disease, anorectal malformations, etc. It is also performed in colorectal surgery to prevent anastomotic leakage, or as an emergency procedure in colonic perforation, injury, etc. Rarely, it is indicated in functional bowel disorders such as constipation or faecal incontinence.[1]

Complete diversion colostomy eliminates luminal contents from the distal portion of colon. The elimination of luminal contents results in changes in colonic environment and motility. Diversion related colitis in defunctionalized colon was described by Morson and Dawson (1972) and Glotzer *et al.* (1981).[2] Colonic restoration after colostomy is commonly associated with multiple functional bowel disorders including constipation, lower abdominal colic, abdominal distension and vague dyspepsia.[1] Residual constipation and erratic bowel movements has been observed following the restoration of bowel continuity after definitive surgery for Hirschsprung's disease.[3] There is a controversy whether short period of diversion colostomy affects bowel motility after restoring continuity or the disease *per se* is responsible for these disturbances. Factors like residual disease, skip lesions, post-pull through ischaemic changes, diversion colitis and defunctionalization could also be responsible for the functional disturbances. By performing colostomy in healthy rats, we eliminated the confounding factors so that the changes in the distal segment of the colon could solely be attributed to the defunctionalization.

The present study focuses on the nitrergic innervation of the colon following colostomy. Nitric oxide (NO) is a final mediator of non-adrenergic, non-cholinergic (NANC) descending inhibitory neurotransmission in the gut. It has been shown that NO released from the nitrergic nerve terminals in the colon initiates inhibitory junction potentials, which cause relaxation of the colonic smooth muscle.[4] Neuronal NO synthase is responsible for the synthesis and release of NO from arginine. The enzyme NADPH diaphorase, which reduces nitroblue tetrazolium (NBT) to an insoluble formazan reaction product, has been colocalized with NOS in the brain and peripheral tissues.[5,6] Complete colocalization of NOS and NADPH diaphorase in the gastrointestinal tract has been reported in

Address for correspondence
Dr A. Shariff, Associate Professor, Department of Anatomy, All India Institute of Medical Sciences (AIIMS), New Delhi 110029 India.
Tel: +91 11 33137531; fax: +91 11 26588663;
e-mail: shariff@aiims.ac.in
Received: 1 November 2003
Accepted for publication: 19 February 2004

many species including man. The analysis of nitrergic neurones may provide clues to explain the disturbances in bowel function after diversion colostomy. This study attempts to evaluate the effect of diversion colostomy on the nitrergic neurones of the myenteric plexus in the defunctionalized colon in rats.

MATERIALS AND METHODS

After obtaining clearance from the Institutional Animal Ethics Committee, 14 adult male Wistar rats were equally distributed into sham surgery and diversion colostomy groups. All the animals received humane care in compliance with the Principles of Laboratory Animal Care and the Guide for the Care and Use of Laboratory Animals formulated and prepared by the Institute of Laboratory Animal Resources and published by the National Institutes of Health (NIH publication no. 86–23, revised 1985).

Diversion colostomy

Diversion colostomy ($n = 7$) was performed under general anaesthesia (ketamine HCl, 50 mg kg^{-1} i.p.) using an operating microscope (Leica, Wetzlar, Germany) with strict asepsis and antibiotic cover (ceftriaxone 1000 mg kg^{-1}). A 2-cm long midline incision was made and the caecum was delivered through this incision and colon was divided 5 cm from the caecum after a window was made in the adjoining mesentery preserving the arterial arcade. A proximal stoma and a distal mucous fistula were created 3 cm apart in the midline, using single-layer, interrupted, seromusculocutaneous sutures (5-O polyglactic acid). This wide separation of the stoma prevented faecal spillage into the distal segment. The abdomen was closed in two layers after instilling 4 mL of sterile normal saline intraperitoneally, to make up for the intraoperative fluid losses. Oral cefixime (6 mg daily) was administered for 2 days postoperatively.

Sham operation

Sham operation ($n = 7$) was performed by a 2-cm midline abdominal incision under general anaesthesia and precautions described above. Caecum and colon were delivered through the incision and returned back to the abdominal cavity. The abdomen was closed as in the diversion colostomy group.

Collection of colonic tissue

All the rats were killed by ether inhalation 45 days after performing diversion colostomy or sham operation. The abdomen was opened and the defunctionalized colon was collected from 1 cm distal to the site of mucous fistula up to the anus in the operated and corresponding parts of the colon in the sham-operated rats and the tissue was kept undisturbed in 0.1 mol L^{-1} phosphate buffer until no visible contractions were seen. The defunctionalized colonic segment was empty. The collected colons of the sham-operated rats were gently cleaned with 0.1 mol L^{-1} phosphate buffer.

Preparation of tissues for NADPH diaphorase histochemistry

Tissues were fixed in 4% paraformaldehyde for 2 h at 4 °C, washed thoroughly in chilled 0.1 mol L^{-1} phosphate buffer and cryoprotected in sucrose at 4 °C for 8 h. The samples were frozen in Optimum cutting temperature (OCT) compound, 20 μm thick cryo-sections were cut and fixed onto slides coated with 1% gelatine and air-dried.

NADPH diaphorase histochemistry

The cryo-sections on the glass slides were washed several times with 0.1 mol L^{-1} phosphate buffer (pH 7.6). NADPH diaphorase activity was rendered visible by incubating the sections in 10 mL, 0.1 mol L^{-1} Tris–Cl buffer (pH 7.8) containing 10 mg β-NADPH, 1 mg NBT and 0.3% Triton X-100 at 30 °C for 45 min to 1 h in the dark. Washing the tissues with chilled 0.1 mol L^{-1} phosphate buffer terminated reactions and the sections were mounted in a mix of glycerol and phosphate buffer (4 : 1). Parallel controls were set up for comparison wherein β-NADPH or NBT was omitted from the reaction buffer.[7]

Masson's trichrome and cresyl violet staining

Serial paraffin sections of the colon (5 μm thick) were cut on a rotary microtome and stained with Masson's trichrome and cresyl violet.

Fluorescent staining for CLSM

One centimetre long segment of colon, fixed for 1 h, was cut open along the line of mesenteric attachment. A laminar preparation of the muscularis externa was made after removing mucosa. Free floating laminar preparations were stained for 2–3 min at room temperature in an extremely dilute (0.001–0.0025% w/v) solution of cresyl violet acetate in distilled water. The preparations were then mounted on glass slides in glycerol with the serosal surface facing up and observed

under Concocal laser scanning microscope (CLSM). Confocal images of myenteric plexus of colon were acquired using a BioRad MRC 1024 laser scanning system (BioRad, NSW, Australia) with a Zeiss Axiophot upright microscope (Zeiss, Hamburg, Germany). Argon/krypton laser was used to excite the fluorophore. Stereological and morphometric methods were used for quantifiable analyses of the light microscopic and confocal images.

Morphometry

Light microscopic images were captured using a Zeiss trinocular microscope with CCD camera connected to a frame grabber card in an IBM-PC. The images were saved as JPEG files with minimum compression and maximum quality. The images were then analysed using ImageJ (developed at the US National Institutes of Health and available at http://rsb.info.nih.gov/ij/).

Morphometry in Masson's trichrome-stained sections

The following parameters were measured:
- Surface epitheliocyte cell height (SECH)
- Distance from bases of the crypts to nearest points on muscularis mucosae.

Morphometry of nitrergic myenteric neurones

More than 400 NADPH diaphorase positive cells were scanned and well-stained cells with proper perikaryon and negatively stained nuclei were chosen for morphometric analysis from each experimental and control animal. The following parameters were measured in 100 randomly chosen formazan positive cells.
- Diameter of cells
- Area and perimeter of soma
- Area and perimeter of nuclei.

Morphometry in cresyl violet stained sections

Area and perimeter of glial cells in the myenteric plexuses were measured using ImageJ (NIH, Maryland, Bethesda, USA).

Stereological methods

Spatial information of the structures can be obtained using appropriate stereological probes. The probes interact with the features in the structure to produce 'events' which are counted or measured. A grid of lines (line probe) was randomly overlaid on the microscopic images in ImageJ. The intersections between the grid lines were used as point probes. The images to be sampled were chosen randomly using a random number generator.

The following parameters were measured using stereological methods:
1 Volume fraction (V_V), of the circular and longitudinal muscle (of the muscularis externa) per unit volume of the gut wall.
2 Volume fraction (V_V) of myenteric nitrergic neurones per unit volume of muscularis externa.
3 Surface density (S_V) of mucosa.
4 Numerical density of neurones in myenteric ganglia using a rectangular 'sampling brick'.
5 Mean calliper diameter ($\langle D \rangle$) of nuclei of neurones.
6 Mean distance between myenteric ganglia.

A brief explanation of the stereological parameters:

Volume fraction (V_V) Volume per unit volume of reference space, a dimensionless ratio.

$$\langle P_P \rangle V_V \tag{1}$$

where, V_V is the volume fraction occupied by the phase [structure(s) of interest] being measured. The brackets '$\langle\rangle$' around P_P signify the expected value for this normalized count, in this case, the point fraction.[8]

Surface density (S_V) Surface area per unit volume, with unit of per μm of a surface.

Estimation of surface density (S_V) was performed as follows:

A line grid was placed on the image. The count of the number of intersections of surface of interest (represented as curves in the section) with the grid lines was normalized by dividing by the total length of line probes to give a line intercept count P_L.

The surface area density $\langle S_V \rangle$ was calculated as:

$$\langle S_V \rangle = 2 \times \text{no. of intersections}/P_L \tag{2}$$

where S_V is the surface area per unit volume of the reference space.

Volume-weighted mean volume (using point sampled intercept length) Combinations of probes can be used to generate useful parameters.[9] The point sampling method[10,11] selected features for measurement in proportion to their volume (points are more likely to hit large than small particles).

The volume of the particle was estimated as follows:

$$V_i = (4/3) \cdot \pi \langle r^3 \rangle \tag{3}$$

$$V_i = \pi/6 \cdot \langle d^3 \rangle, \text{as} \quad d = 2r \tag{4}$$

Numerical density (N_V) The use of tissue sections to count neuronal numbers has many drawbacks

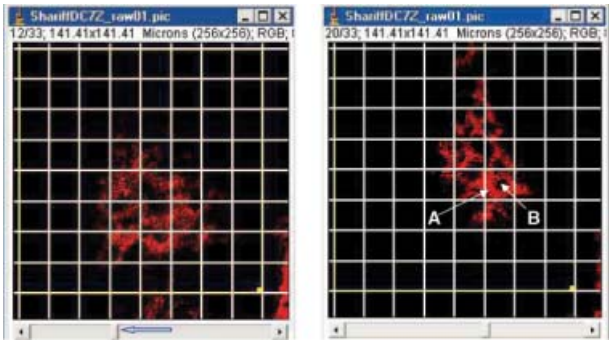

Figure 1 Confocal optical sections of fluorescent Nissl stained myenteric ganglion with a uniform grid overlaid on all the stacks of optical slices to estimate N_V. The nuclei appeared as clearly demarcated negative shadows (B) surrounded by discrete Nissl substance that emitted red fluorescence (A).

including the possibility of sampling bias.[12] Stereology provides a solution for unbiased estimation of particles by introducing the counting rules using 3-D probes, such as the physical disector,[13] optical disector[10,14] and unbiased sampling brick.[15] A grid was overlaid on all slices of the stack of confocal images (Fig. 1). One random slice was considered as the look-up section, and the next slice as the reference section. The separation between the look-up and reference section was kept at one-third the approximate average dimensions of the particles (nuclei in this case) being counted, which ensured that particles are not lost between the sections. The nuclei of the cells that appeared in the reference section but not in the look-up section were counted. Every third slice from the previous reference section was used as the look-up section for the next sampling brick. The ganglion was outlined and the area of the ganglion was estimated at the level of the look-up section and the reference section and an average value obtained. More than 10 measurements were made in each z series (starting with a reference section picked randomly) and several measurements of N_V were obtained from each animal and their mean values were calculated. Neuronal nuclei were not counted if they overlapped the forbidden boundaries of the grid (left and bottom).

The numerical density was obtained in the sampling brick based on the relationship: [16]

$$\langle N_V \rangle = \sum_{i=1}^{n} Q_i \Big/ \sum_{i=1}^{n} P_{i(\mathrm{ref})} \cdot p/a.h \qquad (5)$$

where n is the number of sampling bricks; Q_i, number of particles sampled by ith sampling brick ($i = 1 \ldots n$); P_i, number of points of the p-point grid in the ith frame hitting the reference space ($i = 1 \ldots n$); a, actual area of frame; h, height of sampling brick.

As the estimate of numerical density (N_V) is derived from a density measurement, the effects of processing induced volume changes should be accounted for.[14,17] Prolonged fixation in formalin can produce shrinkage of total volume of tissue; [18] however, in the present study, the colonic tissue was fixed for just 1 h. So, it seems highly unlikely that the estimates have been affected by any shrinkage.

Numerical density (N_A) and mean calliper diameter ($\langle D \rangle$)

The number of nuclear profiles in an optical section at any random level per unit area of the sectional profile of the ganglion is represented as N_A.

$$N_A = \text{no. of nuclei/area}_{\text{ganglion}} \qquad (6)$$

where $\text{area}_{\text{ganglion}}$ is the number of points × separation distance between points.[2]

An estimate of the mean calliper diameter may be obtained using a plane probe sweeping through the three-dimensional structure.[8]

The governing stereological relationship is,

$$N_A = N_V \langle D \rangle$$

Therefore, the mean calliper diameter of the neuronal nuclei, $\langle D \rangle$, was estimated using the formula:

$$\langle D \rangle = N_A / N_V \qquad (7)$$

Mean distance between myenteric ganglia

The mean distance between particles is related to the intercept length of the region between particles. For small features on a 2D plane the mean distance between particles is expressed as $L = 0.5 \times N_A^{-\frac{1}{2}}$ where N_A is the number per unit area.[8]

In the present study, the mean distance between the myenteric ganglia was measured as follows:

$$L = 0.5 \times N_A^{-\frac{1}{2}} \qquad (9)$$

where N_A is the number of ganglia per unit area of muscle (in whole mounts).

Statistical analysis

Statistical analysis was performed by SPSS 10 software. Data was expressed as mean ± SD. Independent sample t-test (Student's t-test) was used to determine the statistical significance between the means. Wherever skewness was present in the data, the raw data was log-transformed and a homogeneous standard deviation was obtained before applying the test of

significance. Standard error of mean (SEM) and the 95% confidence interval (CI) of the difference between the means were noted. For all statistical tests, probability levels of ≤5% were considered to be significant. Chi-squared test was used to evaluate the probability levels of the frequency of distribution of various groups of nitrergic myenteric neurones in the experimental and control groups.

Statistical evaluation of stereological estimates

For a given measurement, stereological estimates were made on a number of fields. The mean values and standard deviations of the counts from the sample of probes selected for measurement were computed. The standard deviation was the basis for estimating the precision of the mean value and deciding whether a sufficient number of fields have been examined.

The precision of the estimates was expressed by the coefficient of error, CE, a measurement of random error introduced by the method due to sampling, noise, counting, and measuring procedures. The purpose was to keep the variation introduced by noise, sampling, counting, and measuring procedures (CE) lower than the biological variation (CV_{biol}) of the tissues under study, where CV is the coefficient of variation. The total variation (CV_{tot}) was expressed as per the equation[10,19,20]

$$CV_{tot}^2 = CV_{biol}^2 + CE^2$$

For all estimates, CV_{tot} is the SD divided by the mean of means (SD/mean). CE was determined as SEM/mean, and CV_{biol} was then calculated from the formula. For a stereological method to be efficient, CE had to be lower than CV_{biol}. The smallest number of sections needed to fulfil this criterion was considered as the optimal sample.

The general linear model repeated measures procedure was used for analysis of variance in a balanced model of the estimates of the numerical density of neuronal cells per unit volume of ganglion. Between-subject factors were specified and the population was divided into two groups, the control and the experimental. Differences were considered to be significant if the value of two-tailed $P < 0.05$.

RESULTS

Gross appearance of defunctionalized colon

The stomas were healthy in all the animals till the day of killing and gross examination showed a marked atrophy of the distal loop of colon. The luminal diameter and wall thickness were markedly decreased uniformly over the whole length of the defunctionalized colon.

Microscopic appearance of colonic tissue

With Masson's trichrome, the mucosa was smooth in appearance with numerous glands or crypts. The muscularis mucosae were stained red and were uniform throughout the section. The muscularis externa was also stained red and an outer longitudinal and an inner circular layers of muscle were discernible.

There was atrophy of all the layers of the distal colon in the defunctionalized group of animals. Small, clear, rounded cells covered the luminal surface and the lamina propria separating individual crypts was more obvious than in the control animals. The surface epitheliocyte cell height ($SECH_{colonic\ epithelium}$) was 6.54 ± 1.296 μm ($n = 711$) in the sham-operated rats and 4.36 ± 1.018 μm ($n = 711$) in the experimental group. The difference was statistically significant ($P < 0.0001$). The distance between the base of the crypt and the nearest point on the muscularis mucosae was measured. This feature was not evaluated in the vicinity of the lymphoid follicles. In the sham-operated rats, this distance ($d_{base\ of\ crypt\ muscularis\ mucosae}$) was 4.46 ± 1.643 μm and 18.81 ± 11.838 μm in the experimental group ($n = 711$). A comparison of the two means showed that there was an extremely significant increase in this distance in the defunctionalized colon. (95% confidence interval, CI = −0.60698 to −0.56082, $P < 0.0001$) (Table 1).

There was no obvious irregularity in the shape of crypts. No mucosal inflammation was detected in the lamina propria of defunctionalized colon. In the defunctionalized colon, the base of the crypt and the muscularis mucosae were occupied by connective tissue fibres and plasma cells or other inflammatory cells could not be detected after careful investigation.

The surface density of the epithelium per unit volume of the colonic mucosa (S_V) was estimated using Weibel's formula, $S_V = 2 \times$ number of intersections of line grids with luminal surface of mucosa/total intercept length.[9,21] In the sham-operated rats, S_V mucosa was 0.0199 ± 0.0113 $\mu m^2/\mu m^3$ (SEM = 0.0013, $n = 70$; CV = 56.78, CE = 6.53%). In the defunctionalized colon, $S_{Vmucosa}$ was 0.0096 ± 0.00751 $\mu m^2/\mu m^3$ (SEM = 0.0008, $n = 70$; CV = 78.22, CE = 9.27 %; $P < 0.0001$) (Table 1).

Both the circular and longitudinal layer of the muscularis externa were reduced in size in the defunc-

Table 1 Diversion colostomy causes atrophy of colonic wall after 45 days of inactivity

	Sham operated		Diversion colostomy		
	Mean ± SD	SEM	Mean ± SD	SEM	95% CI†
SECH (μm)	6.54 ± 1.296	0.048	4.36 ± 1.018*	0.038	2.064–2.307
$d_{\text{crypt-mm}}$ (μm)	4.46 ± 1.643	0.061	18.81 ± 11.838*	0.443	−0.60698 to −0.56082**
S_V ($\mu m^2/\mu m^3$)	0.0199 ± 0.0113	0.0013 CE = 6.53% CV_{biol} = 56.403	0.0096 ± 0.00751*	0.0008 CE = 9.27% CV_{biol} = 77.668	0.007–0.0135
V_V, circ\ muscle (dimensionless)	0.5316 ± 0.163	0.0086 CE = 1.61% CV_{biol} = 30.617	0.1673 ± 0.0993*	0.0052 CE = 3.10% CV_{biol} = 23.351	0.343–0.383
V_V, long\ muscle (dimensionless)	0.2483 ± 0.225	0.012 CE = 4.83% CV_{biol} = 90.48	0.1385 ± 0.03*	0.0016 CE = 1.15% CV_{biol} = 21.629	0.086–0.133

*Two-tailed P value <0.0001; **data log-transformed to obtain homogeneousness of SD; †Confidence interval of the difference between means; CE, coefficient of error, CV_{biol}, biological variation (note CE << CV_{biol}); SEM, standard error of mean; SECH, surface epitheliocyte cell height; V_V, volume fraction; S_V, surface density.

tionalized colon. The volume fraction, V_V, of the circular muscle in the control rats was 0.5316 ± 0.163 (SEM = 0.0086; CV = 30.66, CE = 1.61%) and 0.1673 ± 0.0993 in the experimental (SEM = 0.0052; CV = 59.35, CE = 3.1%). The volume fraction, V_V, of the longitudinal muscle layer of the muscularis externa in the sham-operated rats was 0.2483 ± 0.225 (SEM = 0.012; CV = 90.61, of error, CE = 4.83%) and 0.1385 ± 0.03 in the experimental rats (SEM = 0.0016; CV = 21.66, CE = 1.15%). This diminution in the volume fractions of the circular and longitudinal muscle layers with respect to the total volume of the gut was extremely significant ($P < 0.0001$) (Table 1).

Nitrergic neurones in the myenteric plexus

NADPH diaphorase positive neuronal cells and their processes were found in the myenteric and submucous plexuses throughout the examined segment of colon. A negatively stained nuclear region was seen against the background of dark bluish-black stained cytoplasm. The histochemical reaction visualized a sharp outline of the neuronal perikarya. The population of NADPH diaphorase positive neurones in the myenteric plexus was heterogeneous in terms of cell size. Most of the myenteric neurones were elongated, their long axis being two to three times the short axis and parallel to the circular musculature. Non-neuronal cells such as mucosal epithelium, enteric glial cells (EGC), mast cells, endothelial cells and smooth muscle cells did not take up the stain (Fig. 2A).

The NADPH diaphorase positive neurones were flattened, stellate or angular with numerous lamellar processes extending for short distances from the cell body in the sham-operated animals. Long processes extended from the cell bodies towards other ganglia or smooth muscle layers of the muscularis externa. These neurones resemble the type I Dogiel neurones. Other neuronal cells with smooth oval outline were also seen. Numerous thin long processes extended from these cell bodies (Fig. 2A).

The topographic distribution of various nerve cells and fibres in the experimental group was similar to that observed in sham-operated rats (Fig. 2A, B). Numerous varicosities were present on the nerve fibres within the smooth muscle layers. NADPH diaphorase staining was detected in dense nerve fascicles, forming intra- and inter-ganglionic connections (Fig. 2A, B), suggesting that NO might be released along the whole length of the nerve fibre rather than exclusively at varicose regions.

Morphometry of diaphorase-positive neurones

The mean (±SD) area of the neuronal soma of the nitrergic myenteric neurones was 306.462 ± 147.022 μm (median 277.892 μm^2, range 919.6) in the sham-operated rats and 124.79 ± 71.79 μm^2 in the experimental (95% CI = 0.3808–0.4294,data log-transformed; median 105.8936 μm^2, range 407.68). This diminution in the area of the nitrergic neurones was statistically significant ($P < 0.0001$). The perimeter of the neuronal soma was 78.8969 ± 22.33 μm (median 76.65 μm, range = 37.83) in the control group, and there was a statistically significant ($P < 0.0001$) diminution of the perimeter in the experimental group

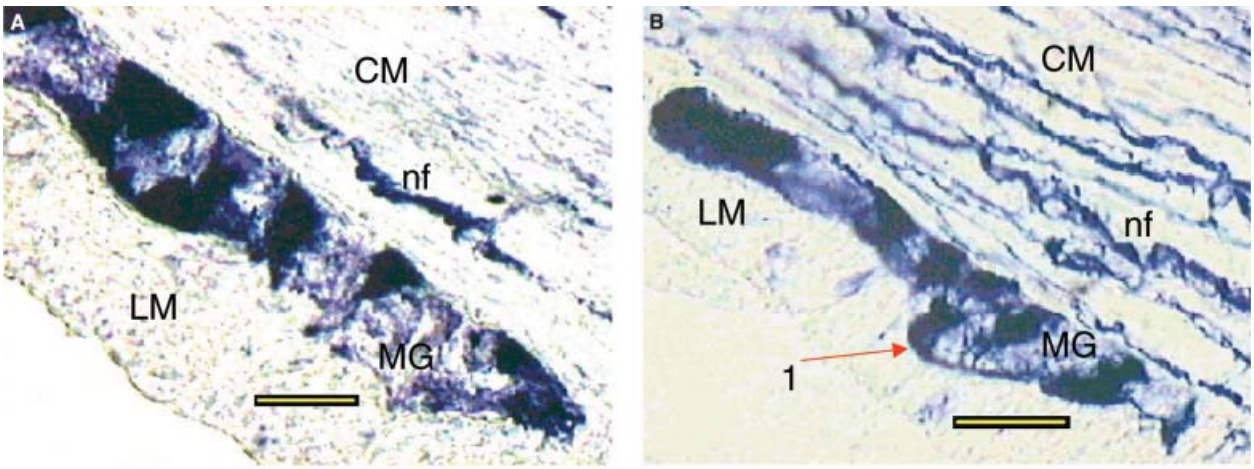

Figure 2 NADPH diaphorase stained light micrographs of myenteric ganglia. Marked reduction in size of neuronal soma and nuclei of nitrergic neurones (1) of myenteric plexus in the defunctionalized colon of rats (B) after diversion colostomy; (A) sham operated, (B) diversion colostomy. Note that the topographic distribution of diaphorase positive nerve cells and fibres was similar in the experimental as well as in sham-operated rats. nf, NADPH diaphorase positive varicose nerve fibres in the circular muscle layer; LM, longitudinal muscle; CM, circular muscle; MG, myenteric ganglia (scale bar 50 μm).

(48.14 ± 14.88 μm, 95% CI = 0.2042–0.2313, data log-transformed; median 46.14 μm, range = 86.11) (Table 2).

The mean (±SD) area of the nuclei of the nitrergic neurones in the sham-operated rats was 55.27 ± 45.13 μm^2 (median 46.86 μ^2m, range = 436.35) and 28.11 ± 16.56 μm^2 (95% CI 0.2652–0.3197, data log-transformed; median 25.18 μ^2m, range = 120.06) in the experimental group ($P < 0.0001$). The nuclear perimeter was 29.649 ± 9.88 μm (median 28.31 μm, range = 88.97) in the sham-operated rat and significantly reduced after diversion colostomy (20.246 ± 6.17 μm, 95% CI = 0.1527–0.1810, data log-transformed; median 20.079 μm, range = 31.50, $P < 0.0001$) (Table 2).

The point sampled intercept probe estimated the volume of the nitrergic neurones in the myenteric plexus. In the control group, the volume of the nitrergic myenteric neurones was 9817.96 ±

Table 2 Diversion colostomy causes atrophy of colonic nitrergic myenteric neurones

	Sham operated		Diversion colostomy		
	Mean ± SD	SEM	Mean ± SD	SEM	95% CI†
Volume-weighted mean volume (μm^3)	9817.96 ± 10323.427	467.319 CE = 4.75%	5131.072 ± 4851.475*	265.46 CE = 5.17%	0.2417–0.3480**
Area of neuronal soma (μm^2)	306.462 ± 147.022 277.892, 919.6‡	5.5569	124.79 ± 71.79* 105.8936, 407.68‡	2.7138	0.3808–0.4294**
Perimeter of neuronal soma (μm)	78.8969 ± 22.33 76.65, 37.83	0.8441	48.14 ± 14.88* 46.14, 86.11‡	0.5669	0.2042–0.2313**
Area of neuronal nuclei (μm^2)	55.27 ± 45.13 46.86, 436.35‡	1.7058	28.11 ± 16.56* 25.18, 120.06‡	0.6262	0.2652–0.3197
Perimeter of neuronal nuclei (μm)	29.649 ± 9.88 28.31, 88.97‡	0.3736	20.246 ± 6.17* 20.079, 31.50‡	0.2334	0.1527–0.1810**
$V_{V\ NO,\setminus\ muscle}$ (dimensionless)	0.0866 ± 0.0434	0.0027 CE = 3.11% CV_{biol} = 50.01	0.0125 ± 0.0121*	0.0006 CE = 4.80% CV_{biol} = 96.68	0.069–0.078

*Two-tailed P value <0.0001; **data log transformed to obtain homogeneousness of SD; †confidence interval of the difference between means; ‡ median, range; CE, coefficient of error, CV_{biol}, biological variation (note CE << CV_{biol}); SEM, standard error of mean; V_V, volume fraction.

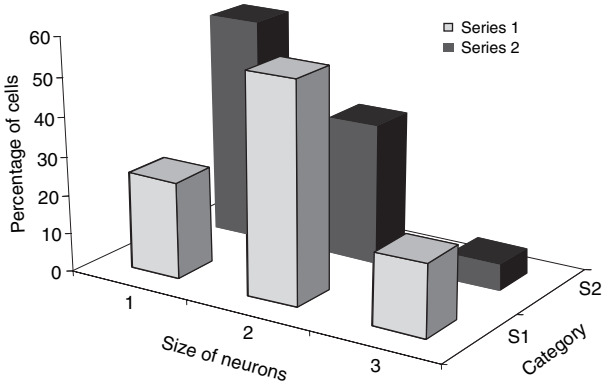

Figure 3 Distribution of nitrergic myenteric neurons based on profile diameters. S1, data from sham-operated rats; S2, data from rats that underwent diversion colostomy. 1, small; 2, medium and 3, large-sized nitrergic myenteric neurones. Note that there is a prominent diminution of the medium and large-sized diaphorase positive neurones in the myenteric plexus of defunctionalized rat colon ($\chi^2 = 158.44$, $P < 0.0001$).

10323.427 μm^2 (mean ± SD; $n = 488$ estimates made in seven animals; median value is 7115.66 μm^2; range = 64679.53; CE = 4.75%). The volume of the nitrergic neurones in the myenteric plexus was significantly reduced in the defunctionalized colon (5131.072 ± 4851.475 μm^2; mean ± SD; $n = 334$ estimates made in 7 animals; median value is 3725.64 μm^2; range = 33865.12, CE = 5.17%; 95% CI = 0.2417–0.3480, $P < 0.0001$) (Table 2).

The mean transverse diameter of the nitrergic neurones in the myenteric plexus was 16.31 ± O.96 μm in the sham-operated rats. This diameter was significantly reduced in the nitrergic neurones of the defunctionalized colon (11.76 ± 3.04 μm, $P < 0.0027$). The mean longitudinal diameter of the nitrergic neurones in the myenteric plexus was 15.66 ± 0.45 μm in the sham-operated rats. This diameter was significantly reduced in the nitrergic neurones of the defunctionalized colon (12.08 ± 3.18 μm, $P < 0.0124$). The sum of the transverse and longitudinal diameter was 31.97 ± 9.55 μm in the nitrergic neurones of the myenteric plexus in the control rats. The sum of the transverse and longitudinal diameter was significantly reduced in the nitrergic neurones of the defunctionalized colon (23.85 ± 10.69 μm, $P < 0.0001$, 95% CI 0.138125–0.175075).

The nitrergic neurones in the myenteric plexus were arbitrarily grouped into three groups based on the sum of their transverse and longitudinal diameter (profile diameters).

Characterization of nitrergic neurones in myenteric plexus: $D = \sum t + l$ where t is the transverse diameter and l, longitudinal diameter. Small neurones: 0–25 μm; medium neurones: 25.1–40 μm; large neurones: >40 μm.

In the sham-operated rats, 24.9% of the nitrergic neurones in the myenteric plexus were small neurones, 56.5% medium-sized neurones and 18.7% were large neurones. In the rats that underwent diversion colostomy, 57.1% neurones were small neurones, 36% neurones were medium-sized neurones and 6.9% neurones were large. These results indicate that after a period of inactivity in the gut, there was a diminution in the population of the large and medium-sized nitrergic neurones in the myenteric plexus of colon ($\chi^2 = 158.44$, $P < 0.0001$) (Fig. 3).

The nitrergic neurones were classified and frequency distribution of cell body and nuclear areas were studied. It was observed that the median cell and nuclear sizes shifted left in the defunctionalized colon, indicating that the process of faecal stream diversion caused significant diminution in these parameters (Figs 4–6).

The volume fraction (V_V) of nitrergic neurones in the myenteric plexus per unit volume of muscularis externa was 0.0866 ± 0.0434 (SEM = 0.0027, CV = 50.11, CE = 3.11%) in the colon of the sham-operated rats. This fraction was significantly reduced in the

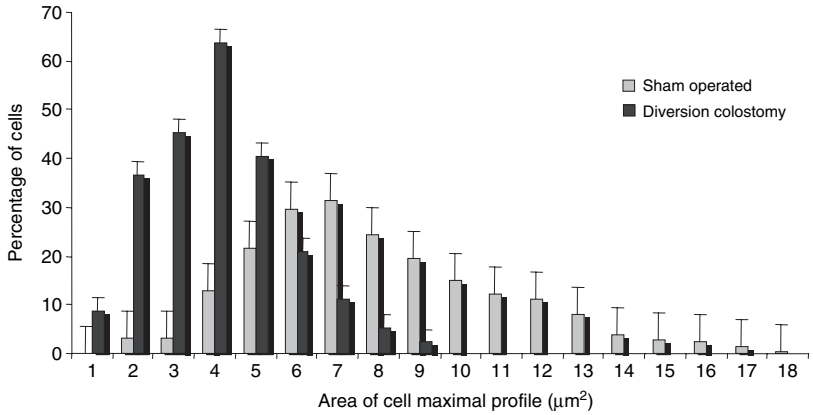

Figure 4 Histogram of nitrergic nerve cell size (mean ± SEM) in myenteric plexus of rat colon based on Fibonacci sequence. A Fibonacci sequence is one in which a given term is obtained from the sum of the two previous terms. The Fibonacci sequence is a natural growth sequence and rises less steeply than an integral logarithmic progression. Note the prominent left shift in the area of the nitrergic neuronal cells obtained from the defunctionalized colon.

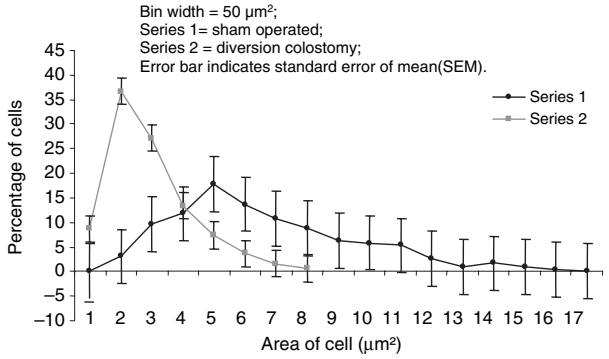

Figure 5 Frequency distribution of mean somatic sizes of NADPH diaphorase positive myenteric neurones. Note the shift of the curve to the left.

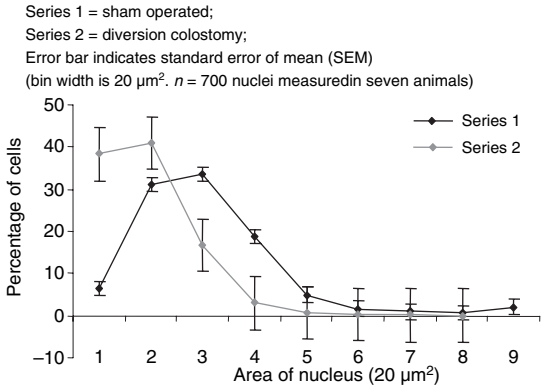

Figure 6 Frequency distribution of mean nuclear profile size in myenteric plexus of rat colon. Note the shift of the curve to the left.

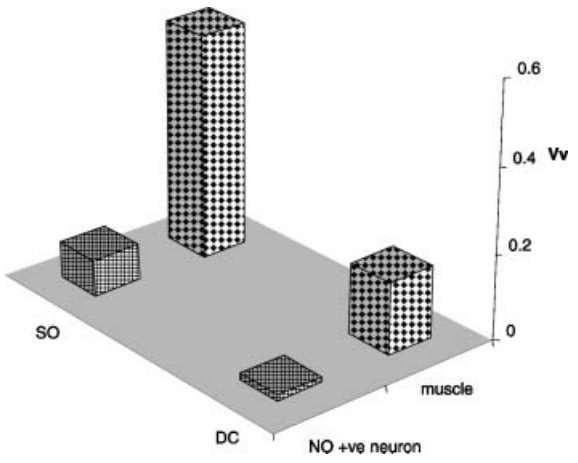

Figure 7 Histogram showing diminution in volume fractions of nitrergic myenteric neurons and smooth muscle cells (SO, sham operated; DC, diversion colostomy).

defunctionalized colon (0.0125 ± 0.0121, SEM = 0.0006, CV = 96.8, CE = 4.8%; $P < 0.0001$) (Fig. 7; Table 2).

Nissl staining

Cresyl violet stained the Nissl substance in the neuronal cells of the myenteric plexus of rat colon. Smaller cell profiles with deeply stained nuclei and clumps of heterochromatin were seen and identified as the EGC. The cytoplasm of glial cells was not usually visible, whereas even the smallest neurones showed a rim of cytoplasm around the nucleus. The size of a glial nucleus is considered to reflect the size of the whole glial cell.[22] The mean areas of the glial nuclei were 7.348 ± 3.84 μm^2 ($n = 352$, seven animals) in sham-operated rats and 5.389 ± 3.17 μm^2 ($n = 352$, seven animals) in the myenteric plexus of the experimental rats. This reduction in the glial nuclear size was extremely significant ($P < 0.0001$). The mean perimeter of the glial nuclei was 10.94 ± 3.09 μm ($n = 352$, seven animals) in sham-operated rats. There was a statistically significant reduction ($P < 0.0001$) of perimeter of the glial nuclei in the experimental group (9.231 ± 2.64 μm, $n = 352$, seven animals) (Table 3).

Fluorescent Nissl staining with cresyl violet

The whole mount preparations and sections of colon (stained with ultra low concentrations of cresyl violet) were viewed under a confocal laser scanning microscope (BioRad MRC1024; BioRad, NSW, Australia). The filter set was same as the one used to detect rhodamine (excitation 568 DF10, emission 585 LP). The neuronal cell cytoplasm emitted a brilliant red fluorescence and a thin optical slice showed the halo of discrete Nissl substance around a central dark nucleus (Fig. 1). Cresyl violet stained the glial nuclei, which appeared as dense fluorescent bodies. Blood vessels in the wall of the gut appeared as negative shadows. A series of optical sectional images of the myenteric ganglia were obtained, and the *z*-step was kept larger than the X–Y resolution.

Numerical density of neuronal cells in myenteric ganglia

The numerical density of the nuclei of neurones in the myenteric plexus was estimated per unit volume of the ganglion. The nuclei were chosen for the feature count as they appear as discrete negatively stained particles and represent the neurones. In the sham-operated rats, the numerical density of the

Table 3 Colostomy affects the neurons and glial cells of myenteric plexus

	Sham operated		Diversion colostomy	
	Mean ± SD	SEM	Mean ± SD	SEM
N_V	19 730 ± 1465		2625 ± 2281	$P < 0.001$(GLM repeated measures ANOVA)
$\langle D \rangle$ (μm)	3.0957 ± 1.3653	0.1719	1.6086 ± 0.3485	0.0439($P < 0.0163$)
L ($L = 0.5N_A^{-\frac{1}{2}}$) ($\mu$m)	12.5416 ± 1.56	0.2604	42.5788 ± 5.467*	0.9112 (95% CI = −0.5565 to −0.5037**)
Glial nuclear area (μm^2)	7.348 ± 3.84	0.2047	5.389 ± 3.17*	0.1689 (95% CI = 1.41–2.45)
Gial nuclear perimeter (μm)	10.94 ± 3.09	0.165	9.231 ± 2.64*	0.141 (95% CI = 1.268–2.121)

*Two-tailed P value <0.0001; **data log-transformed to obtain homogeneousness of SD; N_V, numerical density of myenteric neurones per unit volume of ganglia; $\langle D \rangle$, mean caliper diameter of neuronal nuclei; L, distance between myenteric ganglia; size of glial nuclei is considered to reflect the size of whole glial cell.

neurones in the myenteric ganglion was 19730 ± 1465 neuronal cells per 10^6 μm^3 of the ganglionic volume. In the rats that underwent diversion colostomy, the numerical density of the neurones in the myenteric ganglion was 2625 ± 2281 neuronal cells per 10^6 μm^3 of the ganglion (Table 3). This reduction in the numerical density of the total number of neurones per unit volume of myenteric ganglion was extremely significant ($P < 0.001$, repeated measures ANOVA) (Table 3). This density estimate can be quoted strictly under the assumption that the neuronal cells were statistically homogeneous in the reference space (ganglion). The bricks were positioned randomly and independently of each other without any correlation between the data. This ensured that the estimates of variance between the different sampling bricks were statistically independent.

Additionally, the mean calliper diameter $\langle D \rangle$, of the neuronal nuclei was significantly diminished ($P < 0.001$) in the neurones of the myenteric ganglia of the defunct colon, indicating that there was a diminution in the size of neuronal cells in the myenteric ganglia, 45 days after performing diversion colostomy (Table 3).

In the present study, it was also shown that there was a significant increase ($P < 0.0001$) in the distance between the two myenteric ganglia after diversion colostomy (Table 3). This indicates a decrease in the size as well as the number of myenteric ganglia after a period of inactivity of the colon.

DISCUSSION

Effect of colostomy on colonic wall

The present study demonstrated that exclusion of faecal stream from a segment of colon for 45 days induced significant colonic atrophy, without any inflammation, in the defunctionalized colon. Mucosal atrophy was evident by a significant reduction in SECH and increased distance between bases of the crypts and muscularis mucosae. The surface density of the colonic mucosa in relation to the mucosal volume (S_V) was 51.75% less in the experimental group than in the sham-operated rats. Additionally, there was an extremely significant diminution in the volume fractions (V_V) of both the circular and longitudinal muscle layers after diversion colostomy (Table 1).

Effects of diversion colostomy on nitrergic myenteric neurones

The NADPH diaphorase positive neurones represent NO-synthesizing neurones within the enteric nerve plexuses. There was an extremely significant diminution in the size (area and perimeters) of the neuronal soma and nuclei of nitrergic myenteric neurons in the defunctionalized colon. There is a median distribution of the neuronal size in the rat colon[23] and a shift of the median (of the cell and nuclear area) to the left was observed indicating atrophy of the nitrergic myenteric neuronal cells. There was a significant diminution in the volume-weighted mean volume of the neuronal soma of nitrergic myenteric neurones in the experimental group. There was a significant diminution in the volume fraction of the nitrergic neurones per unit volume of muscularis externa (the targets of these neurones) in the defunctionalized colon. It has been demonstrated that the same compounds acting as NOS inducers (e.g. LPS and IFN-γ) rapidly inhibit the activity of nNOS and decrease the intracellular NO levels in human astrocytoma cells, through tyrosine residue phosphorylation of nNOS.[24] There was no evidence of inflammation in the defunctionalized colon and the changes in the

dimensions of the nitrergic neurones could exclusively be attributed to the diversion of the faecal stream in the present study.

The nitrergic neurones in the myenteric plexus were categorized into small, medium and large neurones, based on their profile diameters.[25] Small, medium and large nitrergic neurones were in a ratio of 24.9 :56.5 : 18.6 in the sham-operated rats and 57.1 : 36 : 6.9 in the experimental group. These results indicated that after diversion colostomy, there was a shift of the cell population towards the small-sized neurones, possibly because of atrophy of the nitrergic neurones or a decrease in the number of the medium and large-sized neurones.

Numerical density (N_V) of myenteric neurones is reduced after colostomy

There was a significant diminution in the numerical density of the neuronal cells in the myenteric ganglia (N_V neurone, ganglion). The distance between the myenteric ganglia was significantly increased in the defunctionalized colon. The CE (an index of the uncertainty of the estimates) was <10% (<5% in most cases) in the estimates of the stereological parameters. The biological variation (CV_{biol}) was much higher than the CE of the estimates. These indicate the precision of the stereological estimates and adequacy of the sampling (Table 1–3).

Biological conclusions based on density measurements are difficult to interpret because it is difficult to know if any changes in the density are the result of an alteration in the attributes (like the number and size) of the particles and/or of the reference volume.[14] There was a significant reduction in the numerical density of the cells in the myenteric ganglia and a significant reduction in the mean calliper diameter of the nuclei of the neuronal cells. This is possible, only if there was a reduction in the size and the total number of neuronal cells of the myenteric ganglia of the defunctionalized colon.

Consequences of structural alterations in nitrergic myenteric neurones

The subpopulation of neurones containing NOS mediates non-cholinergic neuro-neuronal transmission in short descending pathways (3–7 mm) in rats. Other neurones with short descending pathways (about 2 mm) include those using vasoactive intestinal polypeptide and pituitary adenylate cyclase activating peptide as neurotransmitters.[26,27] We analysed the nitrergic myenteric neurones 1 cm distal to the site of colostomy, and there was no chance of including those neurones, which were damaged because of the surgical procedure. The diminution in the size of nitrergic myenteric neurones could only be the result of disruption of normal activity and altered functional state of this colonic segment.

Neuronal survival depends on supply of target derived neurotrophic factors, actions of components of the extracellular matrix, and changes in the neuronal responsiveness to these factors. It is not clear whether intestinal atrophic changes affect survival of enteric neurones or whether they induce change in function or expression of neurotransmitters. There is a continuing debate on the adaptive responses of the enteric nervous system in the atrophic intestine.[28] Ekblad *et al.* (1999) showed that adaptive changes in different populations of neurones occur as a result of intestinal dysfunction after ileal bypass.[28] Such adaptive changes may be a result of atrophy or altered luminal milieu and lack of target-derived nerve growth factors.[29]

Nitric oxide mediates relaxation of smooth muscles of the gastrointestinal tract.[30,31] It has been demonstrated that selective absence of NADPH diaphorase positive nerve fibres in gastrointestinal smooth muscle is responsible for spasticity of the aganglionic segment in Hirschsprung's disease. The marked reduction in cell and nuclear area of nitrergic neurones would possibly decrease the synthesis of calcium-dependent NO in picomolar quantities. In the absence or diminished amounts of ligand (NO), the smooth muscle cell apparatus will inefficiently transduce the NO signal. This may adversely affect the oro-aboral transmission of gut contents after restoration of bowel continuity because of defective receptive relaxation in peristaltic wave.

Effect of colostomy on myenteric glia

It was shown that there was a significant diminution in the area and perimeter of the nuclei of the glial cells in the myenteric plexus, indicating atrophy of the glial cells. Glial cells are an active population in the enteric nervous system and neurone-glia crosstalk plays an important role in maintaining the integrity of the enteric nervous system. The EGC network has trophic functions towards enteric neurones and is implicated in the integration and modulation of neuronal activities.[32] The myenteric environment is particularly challenging and enteric neurones may require high levels of support from EGC.[33,34] Therefore, glial atrophy after faecal stream diversion may have affected all the populations of neuronal cells in the myenteric plexus.

Several 'factors' should be taken into account when considering adaptive changes in the enteric microen-

vironment: neurones, EGC, smooth muscle cells and mucosa. There is an important crosstalk among all these cell populations, and absence of luminal stretching hindered this intercellular communication. This communication may occur at two strata: wiring transmission and volume transmission. Lack of luminal contents in the defunctionalized colon may have led to atrophy of the targets (mucosa and muscle) with concomitant atrophy of all the cells in the myenteric plexus including the nitrergic neurones in the myenteric plexus. Disordered paracrine communication in the form of diminished amounts of glial cell derived neurotrophic factor (as a consequence of glial atrophy), an important factor for neuronal cell survival in the ENS may have further led to neuronal dysfunction.[35,36]

The depletion of bolus could lead to anergy of myenteric neurones, decreased muscle activity, lack of muscle derived trophic factor(s), glial dysfunction and withdrawal of glial support. All these could lead to neuronal dysfunction and threatened neuronal survival in the myenteric plexus.

Summary

Diversion colostomy resulted in atrophy of neuronal soma and nuclei of nitrergic myenteric neurones, diminution in the numerical density of the panneuronal cells, along with a diminution in the mean calliper diameter of their nuclei. Further, there was a diminution in the volume fraction of the nitrergic neurones per unit volume of muscularis externa. These results indicate possible diminution of NO in the defunctionalized colon. The changes in the neuronal phenotype were also associated with significant diminution in the volume fractions of the targets of the neurones of the myenteric plexus viz. the muscularis externa. Mechanical factors play an important role in the maintenance of muscle cell integrity.[37] It seems likely that lack of activity has led to profound changes in the neuronal and glial cells of the enteric nervous system of the defunctionalized colon. The gut is deprived of its intraluminal milieu in several conditions including surgical diversion. Our observations may explain the bowel dysmotility following restoration of bowel continuity after a period of inactivity because of colostomy. We are investigating whether these changes are reversible by restoring the continuity after diversion colostomy in the same animal model.

ACKNOWLEDGMENTS

We thank Drs T.S. Roy, R.D. Mehra, S. Wadhwa and T.C. Nag for their help at various stages of this work. Part of this work has been presented in The Fifth European Paediatric Surgery Association (EUPSA) Conference at Tours, France in May, 2003 and Enteric Nervous System 2003 Conference at Banff, Canada in July 2003 and abstract published in Neurogastroenterology and Motility, **15** (2), April 2003, p. 202. Arun Chaudhury and A. Shariff have equal contribution to this work.

REFERENCES

1 Violi V, Cobianchi F, Adami M, Torri T, Ferraro G, Roncoroni L. Human defunctionalized colon: a histopathological and pharmacological study of muscularis propria in resection specimens. *Dig Dis Sci* 1998; **43**: 616–23.
2 Keli E, Bouchoucha M, Devroede G, Carnot F, Ohrant T, Cugnenc PH. Diversion-related experimental colitis in rats. *Dis Colon Rectum* 1997; **40**: 222–8.
3 Miele E, Tozzi A, Staiano A, Toraldo C, Esposito C, Clouse RE. Persistence of abnormal gastrointestinal motility after operation for Hirschsprung's disease. *Am J Gastroenterol* 2000; **95**: 1226–30.
4 Stark ME, Bauer AJ, Sarr MG, Szurszewski JH. Nitric oxide mediates inhibitory nerve input in human and canine jejunum. *Gastroenterology* 1993; **104**: 398–409.
5 Cracco C, Filogamo G. Quantitative study of the NADPH-diaphorase-positive myenteric neurons of the rat ileum. *Neuroscience* 1994; **61**: 351–9.
6 Santer RM. Survival of the population of NADPH-diaphorase stained myenteric neurons in the small intestine of aged rats. *J Auton Nerv Syst* 1994; **49**: 115–21.
7 Scherer-Singler U, Vincent SR, Kimura H, McGeer EG. Demonstration of a unique population of neurons with NADPH-diaphorase histochemistry. *J Neurosci Methods* 1983; **9**: 229–34.
8 Russ JC, Dehoff RT. Practical Stereology. Plenum Press, New York, 1999.
9 Weibel ER. *Stereological Methods. Volume I, Practical Methods for Biological Morphometry*. London: Academic Press, 1979.
10 Gundersen HJ. Stereology of arbitrary particles. A review of unbiased number and size estimators and the presentation of some new ones, in memory of William R. Thompson. *J Microsc* 1986; **143**: 3–45.
11 Mayhew TM. A review of recent advances in stereology for quantifying neural structure. *J Neurocytol* 1992; **21**: 313–28.
12 Hadzijahic N, Renehan WE, Ma CK, Zhang X, Fogel R. Myenteric plexus destruction alters morphology of rat intestine. *Gastroenterology* 1993; **105**: 1017–28.
13 Sterio DC. The unbiased estimation of number and sizes of arbitrary particles using the disector. *J Microsc* 1984; **134**: 127–36.
14 Braendgaard H, Evans SM, Howard CV, Gundersen HJ. The total number of neurons in the human neocortex unbiasedly estimated using optical disectors. *J Microsc* 1990; **157**: 285–304.
15 Howard V, Reid S, Baddeley A, Boyde A. Unbiased estimation of particle density in the tandem scanning reflected light microscope. *J Microsc* 1985; **138**: 203–12.

16 Tomori Z, Krekule I, Kubinova L. Disector program for unbiased estimation of particle number, numerical density and mean volume. *Image Anal Stereol* 2001; **20**: 119–30.
17 Haug H. History of neuromorphometry. *J Neurosci Methods* 1986; **18**: 1–17.
18 Mouritzen DA. Shrinkage of the brain during histological procedures with fixation in formaldehyde solutions of different concentrations. *J Hirnforsch* 1979; **20**: 115–9.
19 Schmitz C. Towards more readily comprehensible procedures in disector stereology. *J Neurocytol* 1997; **26**: 707–10.
20 Gadeberg P, Andersen H, Jakobsen J. Volume of ankle dorsiflexors and plantar flexors determined with stereological techniques. *J Appl Physiol* 1999; **86**: 1670–5.
21 Finkel Y, Larsson L. Morphometric and functional studies of proximal and distal colon in young and adult rats. *J Pediatr Gastroenterol Nutr* 1987; **6**: 454–9.
22 Gabella G, Trigg P. Size of neurons and glial cells in the enteric ganglia of mice, guinea-pigs, rabbits and sheep. *J Neurocytol* 1984; **13**: 49–71.
23 Gabella G. Neuron size and number in the myenteric plexus of the newborn and adult rat. *J Anat* 1971; **109**: 81–95.
24 Colasanti M, Cavalieri E, Persichini T, Mollace V, Mariotto S, Suzuki H, Lauro GM. Bacterial lipopolysaccharide plus interferon-gamma elicit a very fast inhibition of a Ca2+-dependent nitric-oxide synthase activity in human astrocytoma cells. *J Biol Chem* 1997; **272**: 7582–5.
25 Miranda Neto MH, Molinari SL, Stabille SR, Sant'ana DM, Natali MR. Morphologic and quantitative study of the myenteric neurons of the jejunum of malnourished rats (*Rattus norvegicus*). *Arq Neuropsiquiatr* 1999; **57**: 387–91.
26 Ekblad E, Winther C, Ekman R, Hakanson R, Sundler F. Projections of peptide-containing neurons in rat small intestine. *Neuroscience* 1987; **20**: 169–88.
27 Ekblad E, Alm P, Sundler F. Distribution, origin and projections of nitric oxide synthase-containing neurons in gut and pancreas. *Neuroscience* 1994; **63**: 233–48.
28 Ekelund KM, Ekblad E. Structural, neuronal, and functional adaptive changes in atrophic rat ileum. *Gut* 1999; **45**: 236–45.
29 Ekelund M, Ekblad E. Intestinal adaptation in atrophic rat ileum is accompanied by supersensitivity to vasoactive intestinal peptide, pituitary adenylate cyclase-activating peptide and nitric oxide. *Scand. J Gastroenterol* 2001; **36**: 251–7.
30 Shuttleworth CW, Murphy R, Furness JB. Evidence that nitric oxide participates in non-adrenergic inhibitory transmission to intestinal muscle in the guinea-pig. *Neurosci Lett* 1991; **130**: 77–80.
31 Goyal RK, He XD. Evidence for NO redox form of nitric oxide as nitrergic inhibitory neurotransmitter in gut. *Am J Physiol* 1998; **275**: G1185-92.
32 Cabarrocas J, Savidge TC, Liblau RS. Role of enteric glial cells in inflammatory bowel disease. *Glia* 2003; **41**: 81–93.
33 Giaroni C, De Ponti F, Cosentino M, Lecchini S, Frigo G. Plasticity in the enteric nervous system. *Gastroenterology* 1999; **117**: 1438–58.
34 Bush TG. Enteric glial cells. An upstream target for induction of necrotizing enterocolitis and Crohn's disease? *Bioessays* 2002; **24**: 130–40.
35 von Boyen GB, Reinshagen M, Steinkamp M, Adler G, Kirsch J. Enteric nervous plasticity and development: dependence on neurotrophic factors. *J Gastroenterol* 2002; **37**: 583–8.
36 Peters RJ, Osinski MA, Hongo JA, Bennett GL, Okragly AJ, Haak-Frendscho M, Epstein ML. GDNF is abundant in the adult rat gut. *J Auton Nerv Syst* 1998; **70**: 115–22.
37 Bertoni S, Gabella G. Hypertrophy of mucosa and serosa in the obstructed intestine of rats. *J Anat* 2001; **199**: 725–34.

